Analysis of the Decay Properties of the Q^*

M. S. FARBER, T. FERBEL, P. F. SLATTERY,† AND H. YUTA‡
University of Rochester,§ Rochester, New York 14627
(Received 13 August 1969)

We present the decay characteristics of the low-mass Q^+ enhancement in the $(K\pi\pi)^+$ system which is produced in the reaction $K^+p \to (K\pi\pi)^+p$ at 12.7 GeV/c. When treated as a single resonance, this enhancement has the properties expected for the strange member of an $SU(3)$ meson octet with $J^{PC}=1^{++}$. The resonance position and width of the Q are, respectively, 1260±20 and 180±20 MeV.

INTRODUCTION

THERE has recently been much interest in the properties of low-lying $K\pi\pi$ systems which are produced in high-energy K-p collisions.[1] The production and decay characteristics of the Q, in particular, have been the subjects of extensive studies.[2] While there is still disagreement regarding many important aspects of this problem, there also exists a large volume of data which generally lend support to the following conclusions: (1) The isotopic spin of the Q enhancement is $I=\frac{1}{2}$; (2) the Q decays into both πK^* and $K\rho$; (3) the spin-parity of the Q is favored to be 1^+.

We report on the decay properties of the Q effect as observed in a bubble chamber investigation of K^+p interactions at 12.7 GeV/c. The data presented here represent a 5-events/μb exposure of the 80-in. BNL chamber to rf-separated K^+ mesons.[3] Our analysis is based on 3463 events from reaction (1) and 828 events from reaction (2)[4]:

$$K^+p \to K^+p\pi^+\pi^-, \tag{1}$$

$$K^+p \to K^0p\pi^+\pi^0 \searrow \pi^+\pi^-. \tag{2}$$

These reactions are characterized by profuse resonance production[5] and by a high degree of peripherality.[6] In Fig. 1 we present the $K\pi\pi$ mass spectra for events from reactions (1) and (2). The cross-hatched areas in the histograms remain when events in the $\Delta^{++}(1236)$ bands (1120–1360 MeV) are removed from the original samples of data. These figures show the dominating

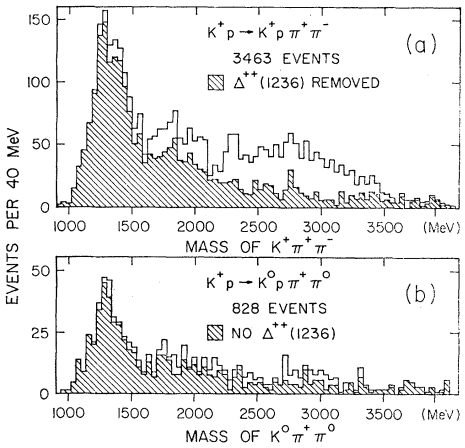

FIG. 1. $(K\pi\pi)^+$ invariant mass for all events from reactions (1) and (2) is shown in (a) and in (b), respectively. The cross-hatched areas represent those events which remain after events in the $\Delta^{++}(1236)$ bands are removed.

* Research supported by the U. S. Atomic Energy Commission. The computer analysis has been made possible by the University of Rochester through a National Science Foundation grant to the University Computer Center.

† A. E. C. Post-Doctoral Fellow.

‡ Presently at Argonne National Laboratory, Argonne, Ill. 60439.

§ Authors hold guest appointments at Brookhaven National Laboratory.

[1] See, for example, the recent reviews by B. French, in *Proceedings of the Fourteenth International Conference on High-Energy Physics, Vienna, 1968*, edited by J. Prentki and J. Steinberger (CERN, Geneva, 1968), p. 91; also articles by G. Goldhaber and A. Pevsner, in *Meson Spectroscopy*, edited by C. Baltay and A. H. Rosenfeld (W. A. Benjamin, Inc., New York, 1968).

[2] Brussels-CERN Collaboration, Phys. Letters **26B**, 30 (1967); Nuovo Cimento **49**, 373 (1967); J. Berlinghieri *et al.*, Phys. Rev. Letters **18**, 1087 (1967); F. Bomse *et al.*, *ibid.* **20**, 1519 (1968); J. Andrews *et al.*, *ibid.* **22**, 731 (1969); J. C. Park *et al.*, *ibid.* **20**, 171 (1967); P. J. Dornan *et al.*, *ibid.* **19**, 271 (1967); D. J. Crennell *et al.*, *ibid.* **19**, 44 (1967); G. Goldhaber *et al.*, *ibid.* **19**, 972 (1967); C. Y. Chien *et al.*, Phys. Letters **28B**, 143 (1968); G. Alexander *et al.*, University of California Radiation Laboratory Report No. UCRL-18872, 1969 (unpublished); M. S. Farber *et al.*, Phys. Rev. Letters **22**, 1394 (1969); C. Y. Chien *et al.*, Phys. Letters **29B**, 433 (1969); Aachen-Berlin-CERN-London (I.C.)-Vienna Collaboration, CERN reports (unpublished); D. R. O. Morrison (private communication); Birmingham-Glasgow-Oxford Collaboration reports (unpublished); D. Colley (private communication); J. C. Park and S. Kim, Phys. Rev. **174**, 2165 (1968); B. C. Shen *et al.*, Phys. Rev. Letters **17**, 726 (1966); J. M. Bishop *et al.*, *ibid.* **16**, 1069 (1966); S. U. Chung *et al.*, Phys. Rev. **182**, 1443 (1969).

[3] H. Foelsche *et al.*, Rev. Sci. Instr. **38**, 879 (1967).

[4] The sample of events from reaction (1) was obtained from the measurement of about 15 000 four-prong events. Of these, approximately 6500 were unselected events, while the remainder were preselected on the scanning table to enrich the yield of low-momentum protons. The events in reaction (2) were not preselected in any way. We estimate that the background from event misidentification is less than 10% in reaction (1) and less than 15% in reaction (2).

[5] In reaction (1), for example, we observe at least 85% resonance production: The cross sections for the production of $\Delta^{++}(1236)$, $K^*(890)$, ρ, and $K^*(1420)$ are, respectively, 390±60, 350±50, 120±40, and 120±30 μb. The $\Delta^{++}(K^{*0}(890)$ and the $\Delta^{++}K^{*0}$-(1420) channels account for only a minor part ($\sim\frac{1}{3}$) of the total K^* production cross sections. The total cross section for reaction (1) is 970±90 μb.

[6] See ref. 2; also, J. C. Berlinghieri *et al.*, Nucl. Phys. **B8**, 333 (1968); J. Bartsch *et al.*, Phys. Letters **27B**, 336 (1968).

presence of the Q effect in the $(K\pi\pi)^+$ mass spectrum at $\sim$1280 MeV; there is also a small shoulder present at the mass of the $K^*(1420)$, as well as a general enhancement in the L region.[7]

In what follows we shall concentrate our attention on the characteristics of the Q as observed in the larger sample of data from reaction (1) and only discuss the events from reaction (2) to demonstrate their over-all consistency with our conclusions. In this analysis we will employ only the cross-hatched events shown in Fig. 1.

SPIN-PARITY AND $SU(3)$ PROPERTIES OF Q (DALITZ-PLOT ANALYSIS)

Figure 2 displays Dalitz plots for the $K\pi\pi$ mass region between 1100 and 1500 MeV for reactions (1) and (2). The data from reaction (1) are shown in 100-MeV mass bands in plots (a), (b), (c), and (d), while the data from reaction (2) are shown in 200-MeV mass bands in graphs (e) and (f). The boundary curves shown on the Dalitz plots indicate the kinematic limits for the central values of the corresponding $K\pi\pi$ mass regions. Clear K^* and ρ bands are observed on these Dalitz plots, particularly at $K\pi\pi$ mass values near the center of the Q peak.[8] There also appears to exist a considerable amount of K^*-ρ overlap for the Q events.

To determine the amount of K^* and ρ structure in the Q, as well as to examine the spin-parity of the Q, we adopted an interference model for Q decay given by Griffiths.[9] Griffiths considers the two-step process of the Q decaying into a pseudoscalar meson and a vector meson, with the subsequent decay of the vector meson into two pseudoscalar mesons. The decay of Q^+ into $(K\rho)^+$ and into $(K^*\pi)^+$ are treated coherently, and the ratio (α) of the amount of ρ amplitude to the amount of K^* amplitude in the decay of the Q is obtained through a maximum-likelihood fit to the Q Dalitz plot.[10] The parameter α, which is determined essentially by the K^*-ρ interference pattern on the $K\pi\pi$ Dalitz plot, describes the charge-conjugation properties (C) of the Q. Consequently, if the Q is a resonance of definite spin-parity, its decay must be characterized by a unique value of α. Furthermore, α can assume only particular values if the Q decay process is $SU(3)$-invariant.

We assumed in our analysis that the Dalitz plot in each $K\pi\pi$ mass interval can be described in terms of an incoherent superposition of a resonant Q, having a unique spin-parity, and a variable amount of uniform $K\pi\pi$ phase space, used to represent the background on the Dalitz plot.[11] Fits were attempted to the data shown in Figs. 2(a)–2(d) for Q spin-parity assignments of $J^P=0^-$, 1^-, 1^+, 2^-, and 2^+. The explicit forms used for the decay matrix elements in treating these J^P values can be found elsewhere[9]; we only give here the matrix element for the $J^P=1^+$ assignment:

$$\frac{d^3\sigma(s,s_1,s_2)}{ds\,ds_1\,ds_2}=\frac{1}{s^{3/2}}|B(s)|^2\sum_{\lambda'}|A_{K^*}{}^{\lambda'}+\alpha A_\rho{}^{\lambda'}|^2,$$
$$A_i{}^{\lambda'}=C_iP_\mu{}^{\lambda'}\cdot\epsilon_\mu{}^\lambda B(s_i)\epsilon_\nu{}^\lambda\cdot(q_j-q_k)_\nu, \tag{3}$$
$$B(s)=1/[s-(M_0+\tfrac{1}{2}i\Gamma_0)^2],$$

where q_j and q_k are the four-vectors of the pseudoscalar mesons from the decay of the vector meson i; $P^{\lambda'}$ and ϵ^λ are polarization four-vectors of the axial Q and the decay vector meson, each having helicities λ' and λ, respectively; s is $(q_1+q_2+q_3)^2$; s_i is the square of the vector-meson rest mass [in the above notation, $s_i=(q_j+q_k)^2$]; B are the mass propagators; C_i are the products of the coupling constants for the two-step decay process; α is a free parameter. In the amplitude A_i, a summation over the indices μ, ν, and λ is understood.

The mass and width of the Q were taken to be, respectively, $M_0=1260$ MeV and $\Gamma_0=180$ MeV (see below for justification). The positions and widths of the vector mesons were taken to be $M_0=765$ MeV and $\Gamma_0=130$ MeV for the ρ, and $M_0=891$ MeV and $\Gamma_0=50$ MeV for the K^*. The fit to the $K\pi\pi$ Dalitz plots consisted of varying the amount of incoherent background and ascertaining the best-fit value of the parameter α. The lowest mass region (1100–1200 MeV) was not very sensitive to the form of the Q-decay matrix element. However, in the mass interval between 1200 and 1500 MeV only the $J^P=1^+$ hypothesis gave consistently adequate χ^2 probabilities for the best fit on the Dalitz plot. The $J^P=0^-$, 1^-, 2^+ hypotheses for the Q yielded extremely poor fits for the entire $K\pi\pi$ mass region. Our results for the $J^P=1^+$ hypothesis and, for comparison, the next best $J^P=2^-$ hypothesis are shown in Table I.

[7] See J. Bartsch *et al.*, Nucl. Phys. **B8**, 9 (1968); also, A. Barbaro-Galtieri *et al.*, Phys. Rev. Letters **22**, 1207 (1969), and references to previous work given in these papers.

[8] Ignoring $K^*\rho$ interference effects, we find that the fraction of ρ and $K^*(890)$ in the Q peak region (1.2–1.4 GeV) is $\sim\frac{1}{2}\rho$ and $\frac{3}{2}K^*$ for reaction (1) and $\frac{1}{2}\rho$ and $\frac{1}{2}K^*$ in reaction (2). The Q^+ production cross section is 190 ± 40 μb in both reactions.

[9] We have used the program COMPLOT written by D. Griffiths. The model is a generalization of the work of W. R. Frazer *et al.*, Phys. Rev. **136**, 1207 (1964). See D. Griffiths, Wayne State University Report, 1968 (unpublished).

[10] We examined the possibility of a complex rather than just a real value for α but found that this extra degree of freedom did not materially improve the quality of our fits. The reality of α implies an interference between the $(K\rho)^+$ and $(K^*\pi)^+$ amplitudes in Q decay.

[11] We also added a small amount of incoherent $K^*(1420)$ amplitude in our fit to the Dalitz plots. We assumed F-type $SU(3)$ couplings in the decay of $K^*(1420)$ into $K\rho$ and $\pi K^*(890)$; see Ref. 9 for details on this procedure. We measured the cross section for $K^*(1420)$ production in the reaction $K^+p\to K^0\pi^+p$ to be 30 ± 7 μb. On the basis of this measurement and the Review of Particle Properties values [Particle Data Group, Rev. Mod. Phys. **41**, 109 (1969)] for the $K^*(1420)$ branching rate in $K\pi\pi$, we expected to observe $\sim$70 $K^*(1420)$ events in the cross-hatched mass spectrum in Fig. 1. A fit to this mass spectrum (to be discussed in the text) indicates that $\sim$120 events are required for the $K^*(1420)$. Since the latter number is not inconsistent with the poorly known $K^*(1420)$ branching rates, we used our best experimental value of 120 $K^*(1420)$ events in the fits to the Dalitz plots. We wish to point out, however, that these fits are not at all sensitive to these small admixtures of $K^*(1420)$ signal.

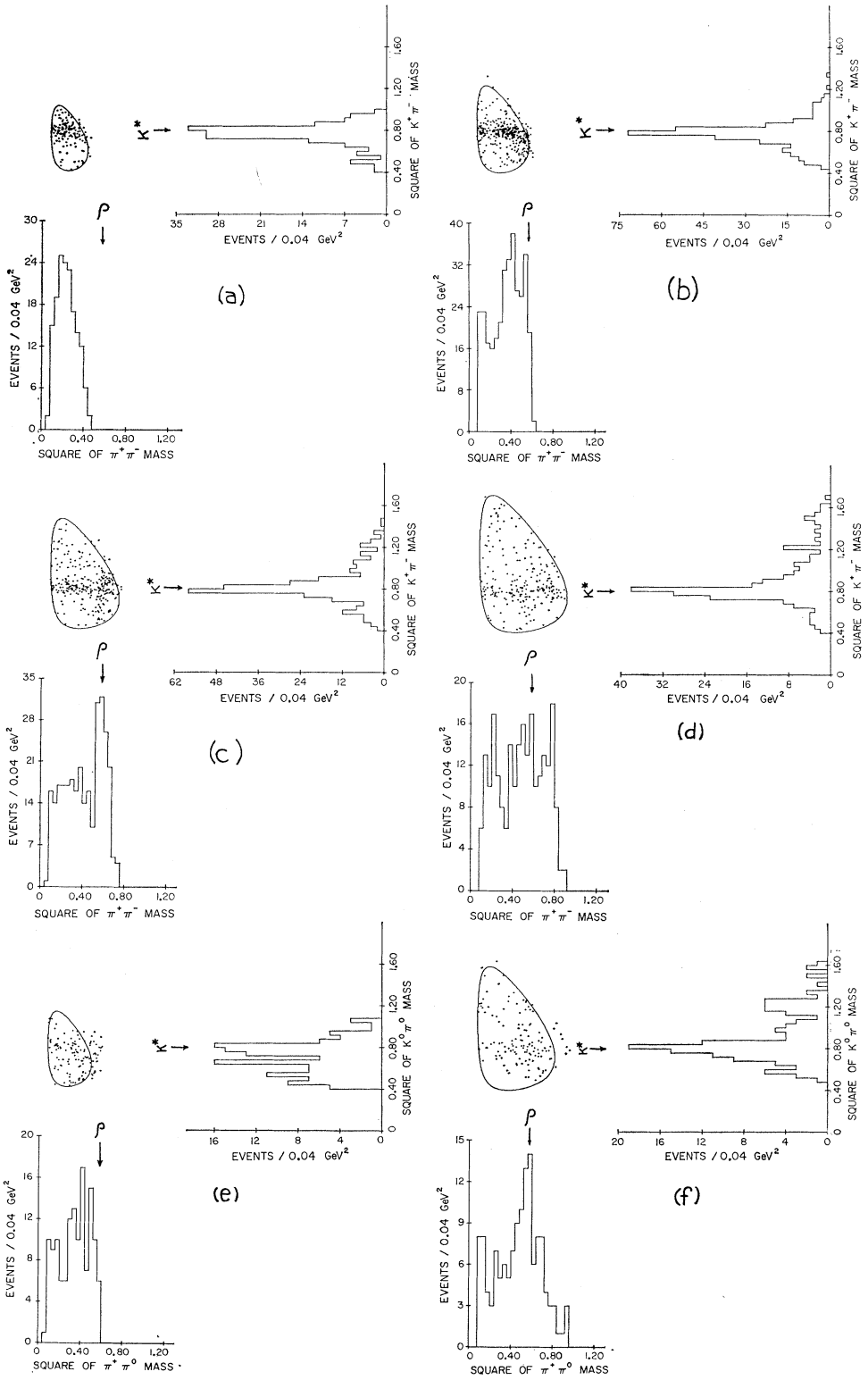

FIG. 2. $K\pi\pi$ Dalitz plots for $K\pi\pi$ invariant masses between 1100 and 1500 MeV. Events from reaction (1) appear in Figs. 2(a)–2(d) in 100-MeV-wide $K\pi\pi$ mass bands. Events from reaction (2) are displayed in (e) and (f) in 200 MeV-wide $K\pi\pi$ mass bands.

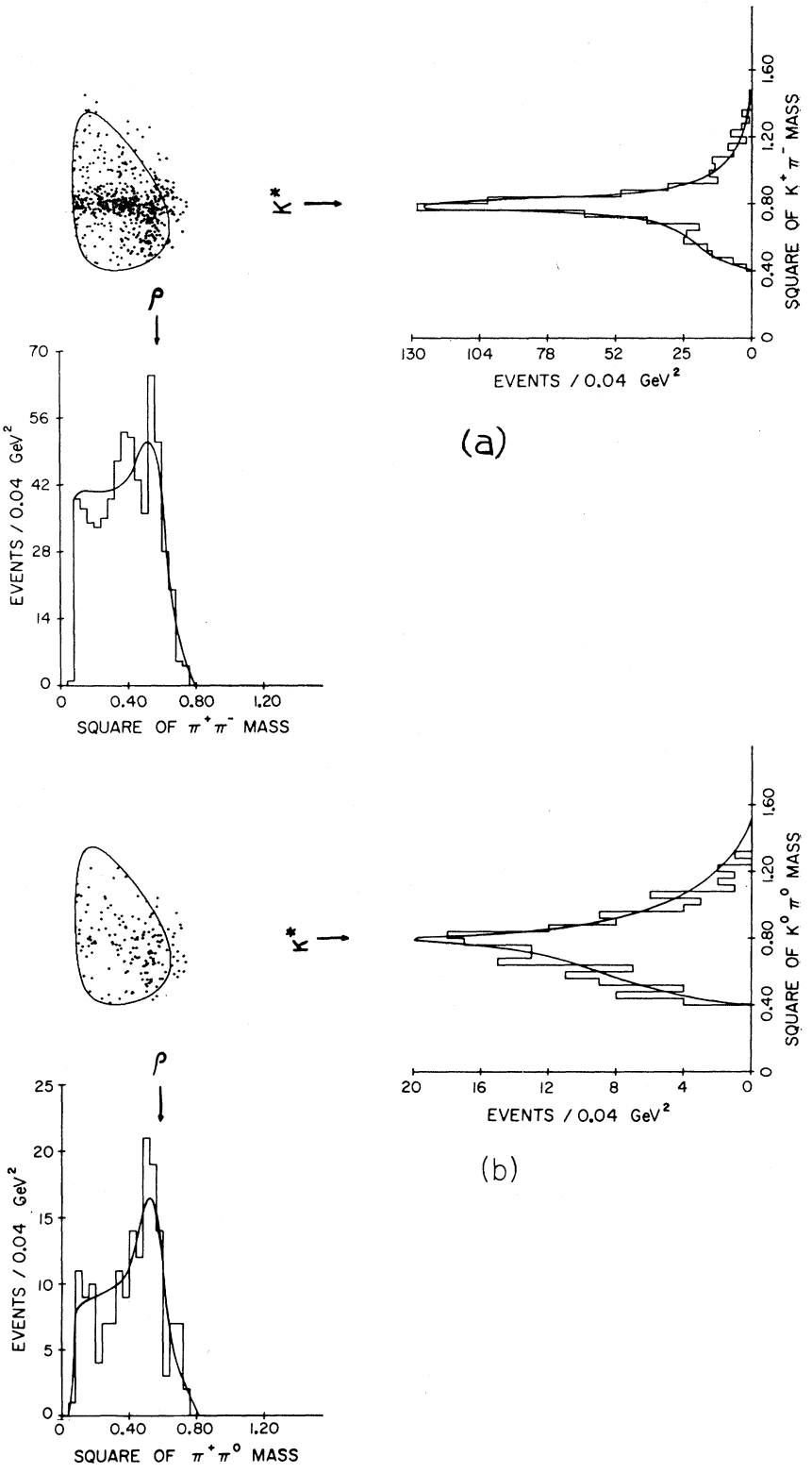

FIG. 3. $K\pi\pi$ Dalitz plots for $K\pi\pi$ invariant masses between 1200 and 1400 MeV. Events from reaction (1) appear in (a); events from reaction (2) appear in (b). For explanation of curves see text.

TABLE I. Results of the Dalitz-plot analysis of reaction (1).

J^P	$K\pi\pi$ mass range (GeV)	No. of events	α	% background[a]	χ^2 probability for fit on Dalitz plot
1^+	1.1–1.2	159	-0.6 ± 0.6	20 ± 10	0.80
	1.2–1.3	328	-1.4 ± 0.2	22 ± 10	0.08
	1.3–1.4	294	-1.1 ± 0.4	33 ± 10	0.25
	1.4–1.5	231	-0.9 ± 0.5	45 ± 10	0.15
	1.2–1.4	622	-1.2 ± 0.2	30 ± 8	0.03
2^-	1.1–1.2	159	1.3 ± 0.9	20 ± 10	0.40
	1.2–1.3	328	-2.5 ± 0.4	10 ± 10	3×10^{-5}
	1.3–1.4	294	-1.5 ± 0.4	30 ± 10	0.04
	1.4–1.5	231	0.8 ± 0.5	50 ± 10	0.03
	1.2–1.4	622	-2.0 ± 0.3	25 ± 8	2×10^{-4}

[a] A fixed additional amount of $K^*(1420)$ was added incoherently in the fits to the Dalitz plots. This contribution was negligible for $K\pi\pi$ masses below 1.3 GeV, and corresponded to 6% of the events in the 1.3- to 1.4-GeV region and 22% of the events in the 1.4- to 1.5-GeV $K\pi\pi$ mass range (see Ref. 11).

Considering the simplicity of our model, we believe that the quality of our fit to the 1^+ hypothesis is acceptable. The value of α for $J^P=1^+$ appears not to vary with the $K\pi\pi$ mass and is consistent with the value $\alpha=-1.0$ which is expected on the basis of the F-type coupling in the decay of the Q; that is, if the Q belongs to an $SU(3)$ octet, then it has $C=+1$.[12]

Figure 3 displays the Dalitz plots for the central bands of the Q region (1200–1400 MeV) for reactions (1) and (2). On the two-body mass projections shown in (a), we give the results of our best fit to the data for reaction (1). A separate fit to the data from reaction (2) was not attempted because of the small number of events in that final state. On the projections in Fig. 3(b)

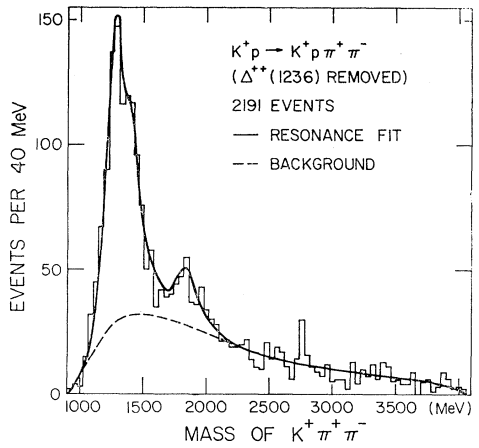

FIG. 4. $K^+\pi^+\pi^-$ invariant mass spectrum for events outside of the $\Delta^{++}(1236)$ mass region. For explanation of curves, see text.

[12] A generalized C parity can be defined for a boson belonging to an $SU(3)$ octet. In our case, the F-type coupling corresponds to $C=+1$ and the D-type of octet coupling corresponds to $C=-1$ for the nonstrange, isotopic spin $=1$ neutral member of the octet. Thus our result for α would classify the Q in the same octet as the A_1. We wish to point out that we introduced a 20% correction in the couplings C_i in expression (3) because of the known $SU(3)$ breaking in the 1^- vector-meson octet; namely, since the ratio of the widths of the ρ and the $K^*(890)$ is not that predicted by $SU(3)$, we explicitly corrected the C_i by this amount of $SU(3)$ breaking. See the procedure suggested by D. Griffiths in Ref. 9.

we show, therefore, the distributions expected for reaction (2) on the basis of the parameters obtained in the fits to reaction (1). The agreement between these predictions and the data are clearly excellent,[13] thus lending further support to our conclusion that the quantum numbers of the Q are $J^{PC}=1^{++}$.[14]

We also examined the effect on the $K\pi\pi$ mass spectrum of the 1^+ fit to the $K\pi\pi$ Dalitz plot. In Fig. 4 we repeat the data presented in the cross-hatched region of Fig. 1(a). The smooth curve represents the best fit to the $K\pi\pi$ mass spectrum (M) using the expression

$$\frac{d\sigma(M)}{dM}=\sum_{n=1}^{4}a_nM^n+\sum_{i=1}^{2}\frac{N_i\Gamma_i/2\pi}{(M-M_i^0)^2+\frac{1}{4}\Gamma_i^2}+N_QG(M). \tag{4}$$

The first term given in (4) is a fourth-order polynomial in the $K\pi\pi$ mass; this type of parametrization was considered as adequate for the representation of the incoherent background in the data. The parameters a_n were allowed to vary freely in the fit. The second term in expression (4) consists of two simple Breit-Wigner forms that were introduced in order to take account of the $K^*(1420)$ signal and the L enhancement in the data. Because of the small contribution of the $K^*(1420)$ and of the L to the total cross section $\sigma(M)$, only the number of resonance events N_i were allowed to vary in the fit; the positions and widths were taken as $M_0=1420$ MeV, $\Gamma=100$ MeV for the $K^*(1420)$, and $M_0=1830$ MeV, $\Gamma=150$ MeV for the L.[15] The final term in expression (4) represents the contribution of the Q. $G(M)$ is a modified Breit-Wigner term (normalized to unity) which has folded into it the phase space and the matrix element for the 1^+ decay of the Q into πK^* and $K\rho$.[16] The number of resonance events N_Q, as well as the

[13] The same percentage of phase-space background and $K^*(1420)$ was used in the comparison of the model with reaction (2) as was found necessary in our fit to reaction (1). $SU(2)$ was assumed to hold in relating π^+K^{*0} to π^0K^{*+} decay. The over-all agreement on the Dalitz plot was superior to that found in reaction (1); this was presumably because of poorer statistics in reaction (2).

[14] In a similar analysis of 7-GeV/c K^+p data, a value of α was found which agreed very well with the prediction of F-type decay for the Q [C. Y. Chien *et al.*, Phys. Letters **28B**, 143 (1968)]. The same $SU(3)$-consistent value for α was also obtained in a study of 12.6-GeV/c K^-p data [see T. Ludlum, thesis, Yale University, 1969 (unpublished)]. A new measurement of α in 9-GeV/c K^+p data, however, gives a value inconsistent with the predictions of $SU(3)$ [G. Alexander *et al.*, University of California Radiation Laboratory Report No. UCRL-18872, 1969 (unpublished)]. This result is particularly interesting in view of our present findings. If α is indeed a function of the beam energy, then a simple $J^{PC}=1^{++}$ interpretation for the Q enhancement is clearly not permissible.

[15] This is not intended to be a measurement of the position and width of the L; these parameters were simply chosen as an adequate representation of the L peak. The L cross section obtained in this manner is ~30 μb.

[16] $G(M)$, where $M=s^{1/2}$, equals $s^{1/2}\int[d^3\sigma/ds ds_1 ds_2]ds_1 ds_2$ as given in expression (3) above. The effect of this matrix element coupled with that of phase space is to shift the observed mass peak from the input value $M_0=1260$ to 1280 MeV, as well as to enhance the high-mass part of the Q. We did not try a similar fit to the data from reaction (2) because of the poor statistics. However, we point out that a larger shift in the observed mass peak of the Q is expected in reaction (2) because of the greater contribution of the ρ in that final state [this is indeed observed in Fig. 1(b)].

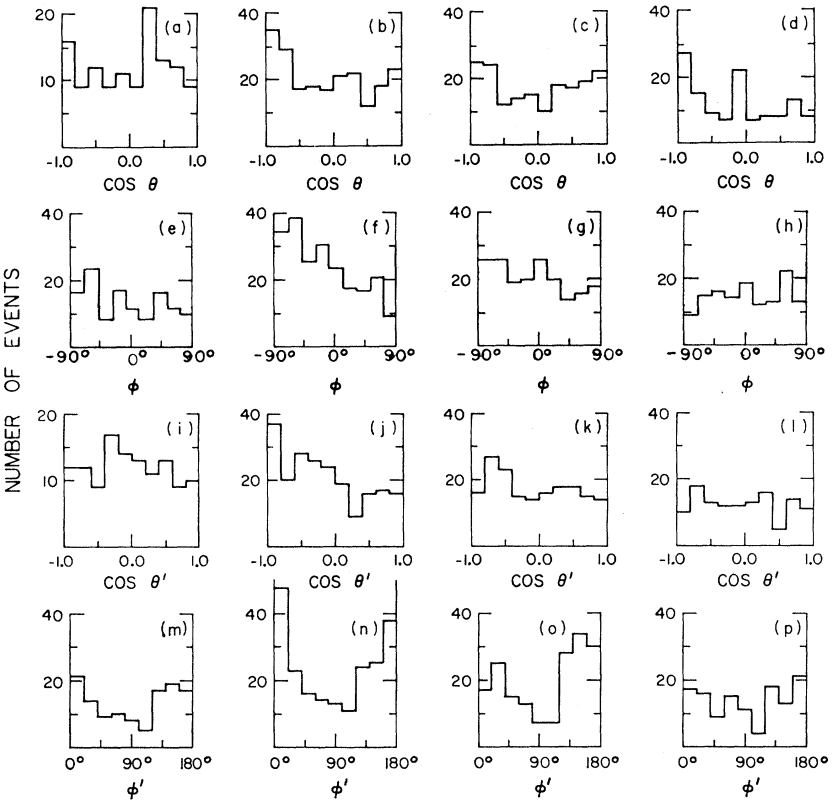

FIG. 5. Angular distributions for $\pi^+K^{*0}(890)$ events from reaction (1). Angles θ and ϕ are the Berman-Jacob angles of the $K^*(890)$ in the $\pi^+K^{*0}(890)$ system's rest frame, while θ' and ϕ' are the angles of the K^+ in the $K^*(890)$ helicity frame. The distributions are for 100-MeV-wide π^+K^{*0} mass regions between 1100 MeV (left) and 1500 MeV (right).

position and width of the Q, were varied in the fit to the mass spectrum of Fig. 4. The best fit to the mass spectrum was obtained using a resonance mass $M_Q=1260\pm20$ MeV, and a width of $\Gamma_Q=180\pm20$ MeV. The amount of $K^*(1420)$ obtained from this fit (120 events) was the same amount which was added incoherently to the background in the fit to the $K\pi\pi$ Dalitz described earlier in this paper.[11] The amount of polynomial background obtained in the Q region (dashed curve in Fig. 4) is clearly consistent with that obtained in the fit to the Dalitz plot (see Table I). The good quality of the fit in Fig. 4 again lends confidence to our conclusion regarding the properties of the Q.

ANGULAR DECAY PROPERTIES

An alternative method for measuring the spin-parity of a boson which decays into a vector meson and a pseudoscalar meson has been suggested by Berman and Jacob.[17] Although this formulation does not apply to regions of the Dalitz plot where there are overlapping vector-meson bands, we have nevertheless followed the suggested procedure and attempted to compensate for the effect of the overlapping bands through a background subtraction technique.[18]

Figure 5 displays the four angles relevant to the π^+K^{*0} decay of the Q^+ in reaction (1). The angles θ and ϕ are the polar and azimuth angles of the K^* in the Q rest frame, while θ' and ϕ' are the angles of the K^+ in the K^* helicity frame.[19] The angular distributions are given as a function of the $K^*\pi$ invariant mass (the K^* band is defined to span 840–960 MeV). The four $K^*\pi$ mass intervals are each 100 MeV wide, starting at a mass of 1100 MeV for the left plots and ending at 1500 MeV for the rightmost plots in the figure.

The distributions in θ and ϕ exhibit small asymmetries; these asymmetries may be due to interference of the πK^* decay mode of the Q with background amplitudes. The ϕ' spectrum shows definite structure ($\sim\cos^2\phi'$) characteristic of helicity $=1$ for the K^* (this excludes the 0^- assignment for Q).[17] The θ' distribution, particularly for the central $K^*\pi$ mass bands, shows an excess of events near $\cos\theta'=-1$; this can be understood

[17] S. M. Berman and M. Jacob, Stanford Linear Accelerator Center Report No. 43, 1965 (unpublished). Our BJ value in Table II is to be identified with the weighted average given in Eq. (2.12) in their paper.

[18] This subtraction technique involved the analysis of the angular correlation for events outside as well as inside the K^* mass band. The various averages of interest were then corrected for the presence of the $K\rho$ channel through a simple method of incoherent subtraction. Since these corrections were generally small, this procedure may yield at least an approximately correct result. We did not attempt to carry out this procedure for events from reaction (2) because of the lower statistics and because of the additional complication presented by the existence of a second K^* band.

[19] The angles θ, ϕ, θ', and ϕ' are defined exactly as given in Ref. 17. For determining θ and ϕ, the z axis is defined by the beam momentum, while the x axis is given by the normal to the Q production plane ($\mathbf{P}_{K\text{in}+}\times\mathbf{P}_{p\text{in}}$), both calculated in the Q rest frame. The angles θ' and ϕ' are obtained in the K^* rest frame, where the z' axis is given by the direction of the K^* in the Q rest frame (helicity axis) and the y' axis is defined by the normal to the K^* production plane ($\mathbf{P}_{K^*}\times\mathbf{P}_{K\text{in}+}$).

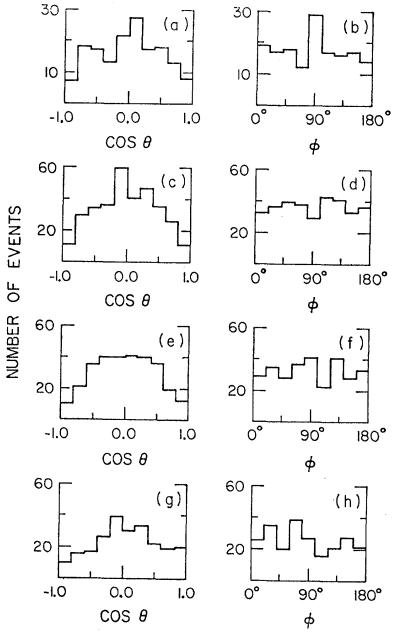

FIG. 6. Angular distributions of the normal to the $K^+\pi^+\pi^-$ decay plane (z axis is the K^+ beam momentum). The distributions in θ and ϕ are for 100-MeV-wide $K^+\pi^+\pi^-$ mass intervals between 1100 MeV (top) and 1500 MeV (bottom).

on the basis of the presence of some ρ in the K^* band. Furthermore, the presence of a large isotropic component in $\cos\theta'$ indicates that there is a substantial amount of helicity=0 state for the K^*, thus immediately excluding the 1^-, 2^+, 3^-, ... assignments for the Q spin parity.[17]

Berman and Jacob suggest a particular series of weighted averages over the angles θ, ϕ, θ', and ϕ' in order to determine the spin-parity of the parent boson. Table II summarizes our results for this procedure. The entry under "BJ value" should be 0 for $J^P=0^-$, $+2$ for $J^P=1^+$ and 2^+, and -2 for $J^P=1^-$ and 2^-. We note that throughout the Q region the BJ value is positive and in the central mass region of the Q it is consistent only with the $J^P=1^+$ and 2^+ assignments. A similar procedure was followed for the $K^+\rho^0$ decay of the Q^+ and we found in this case that the BJ value $=1.81\pm0.44$, again consistent only with the $J^P=1^+$ or 2^+ assignments for the Q.

Both of these results are therefore quite consistent with those obtained in the analysis of the $K\pi\pi$ Dalitz plot. The two techniques are, of course, not independent, but these reactions are nevertheless sufficiently complicated that it is useful to examine them in as many ways as possible.

TABLE II. Results of the Berman-Jacob analysis for π^+K^{*0} events in reaction (1).

$K^*\pi^+$ mass interval (GeV)	BJ value[a]
1.1–1.2	0.76 ± 0.30
1.2–1.3	2.13 ± 0.60
1.3–1.4	4.30 ± 3.10
1.4–1.5	0.93 ± 0.50
1.2–1.4	2.47 ± 0.60

[a] Corrected for background (see Ref. 18).

TABLE III. Results of the examination of the angular distribution of the normal to the $K^+\pi^+\pi^-$ decay plane.

$K\pi\pi$ mass range (GeV)	Value of $\rho_{0,0}$[a]
1.0–1.1	0.80 ± 0.18
1.1–1.2	0.74 ± 0.11
1.2–1.3	0.94 ± 0.06
1.3–1.4	0.93 ± 0.07
1.4–1.5	0.74 ± 0.13
1.2–1.4	0.94 ± 0.05
Momentum transfer[b] $p\to p$ (GeV^2)	Value of $\rho_{0,0}$
<0.03	1.14 ± 0.10
0.03–0.06	0.97 ± 0.10
0.06–0.12	0.83 ± 0.10
0.12–0.24	0.86 ± 0.09
0.24–0.50	1.11 ± 0.14

[a] See Ref. 21 for obtaining $\langle Y_{2,0}(\theta,\phi)\rangle$.
[b] These results are for the central Q band (1200–1400 MeV).

PRODUCTION PROPERTIES OF Q

The angular distributions of the normal to the $K^+\pi^+\pi^-$ decay plane are shown in Fig. 6. The z axis is given by the beam momentum vector as seen in the $K^+\pi^+\pi^-$ rest frame, and the y axis is defined by the normal to the production plane. The angles θ and ϕ are presented as a function of the $K\pi\pi$ invariant mass. The four $K\pi\pi$ mass intervals are each 100 MeV wide, starting at a mass of 1100 MeV for the topmost graphs and ending at 1500 MeV for the graphs at the bottom of the figure. The distributions in ϕ are consistent with isotropy. The θ distributions, particularly in the 1200–1400-MeV $K\pi\pi$ mass region, show a characteristic $\sin^2\theta$ dependence which is indicative of a dominant $J_z=0$ term for Q production.[20]

Assuming the 1^+ spin-parity assignment for the Q region,[21] we have examined the variation of the diagonal density matrix element $\rho_{0,0}$ as a function of the $K\pi\pi$ mass and as a function of the momentum transfer from the beam K^+ to the Q.[22] Table III summarizes our results. The large values observed for $\rho_{0,0}$ are consistent with the diffractive nature of Q production.[23]

OTHER PROPERTIES OF Q

There is no evidence for any resonancelike fine structure in the $K^0\pi^+\pi^+$ mass spectrum [Fig. 7(a)] for the

[20] We calculated the expectation values of all the $Y_{l,m}(\theta,\phi)$ moments up to $l=4$. Only the $Y_{2,0}(\theta,\phi)$ moment was significantly different from zero for $K\pi\pi$ mass below 2 GeV.

[21] For the general form of the angular distribution for the decay of a 1^+ state, see J. D. Jackson, *Les Houches Lectures, Grenoble University* (Gordon and Breach, Science Publishers, Inc., New York, 1965), p. 327.

[22] For the $J^P=1^+$ decay, $\rho_{0,0}=\frac{1}{3}[1-4(5\pi)^{1/2}\langle Y_{2,0}(\theta,\phi)\rangle]$ (see Ref. 21).

[23] See, for example, M. Ross and Y. Y. Yam, Phys. Rev. Letters **19**, 546 (1967).

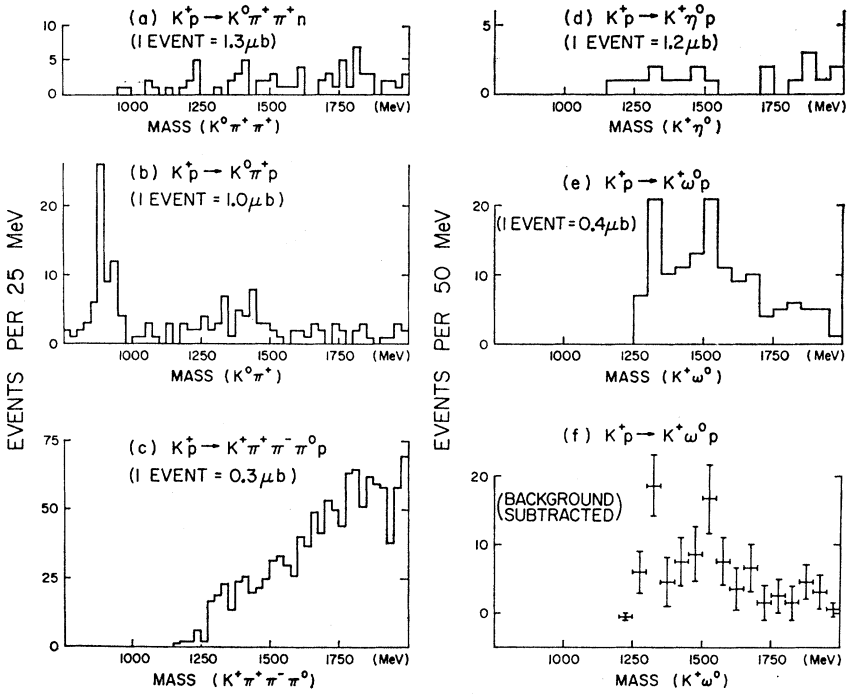

FIG. 7. Mass distributions for $K^0\pi^+\pi^+$, $K^0\pi^+$, and $K^+\pi^+\pi^-\pi^0$ systems in the reactions $K^+p \to K^0\pi^+\pi^+n$, $K^+p \to K^0\pi^+p$, and $K^+p \to K^+\pi^+\pi^-\pi^0p$ are given in (a), (b), and (c), respectively. Graphs (d) and (e) give the $K^+\eta^0$ and $K^+\omega^0$ mass spectra for the events in graph (c). The μb equivalents specified in the figures take account of all unobserved decays of the K^0, ω^0, and η^0. The $K^+\omega^0$ mass spectrum in (f) is obtained after a background subtraction (see Ref. 24).

final state

$$K^+p \to K^0n\pi^+\pi^+ \quad (5)$$
$$\searrow$$
$$\pi^+\pi^-,$$

and we place an upper limit of 7 μb for Q^{++} production in reaction (5). There is, furthermore, no evidence [Fig. 7(b)] for Q^+ decay into $K^0\pi^+$ ($<10\,\mu$b).

The $K^+\pi^+\pi^-\pi^0$ mass spectrum [Fig. 7(c)] for the reaction

$$K^+p \to K^+\pi^+\pi^-\pi^0p \quad (6)$$

does not appear to exhibit any significant enhancements near the mass of the Q^+. The $K^+\eta^0$ mass distribution in Fig. 7(d) for these events shows no indication of a Q^+ decay rate into $K^+\eta^0$, and, accordingly, we place an upper limit of 8 μb for this decay channel (the μb equivalent given in the graph has been corrected for the neutral decays of the η^0).

In Fig. 7(e) we display the $K^+\omega^0$ invariant-mass distribution for events from reaction (6). Here there does appear to be a small enhancement near threshold for the $K^+\omega^0$ system. In Fig. 7(f) we show the $K^+\omega^0$ mass distribution after performing a background subtraction.[24] If the peak at the $K^+\omega^0$ threshold is interpreted as a Q^+ decay in $K^+\omega^0$, then the cross section for this process (including neutral decays of the ω^0) is 10 ± 6 μb. This possible $Q^+ \to K^+\omega^0$ production rate is to be compared with a Q^+ production cross section of 190 ± 40 μb in reactions (1) and (2).

CONCLUSION

We draw the following conclusion from our examination of the production and decay properties of the low-mass $K\pi\pi$ enhancement: The entire phenomenon at our energy can be understood in terms of (1) the Q effect, a $J^{PC}=1^{++}$ resonance having a mass of 1260 ± 20 MeV and a width of 180 ± 20 MeV, and (2) the $K^*(1420)$, which appears as a small shoulder on the high-mass side of the Q peak.

ACKNOWLEDGMENTS

We thank Dr. B. Forman, Dr. A. C. Melissinos, and Dr. T. Yamanouchi for their contributions in the early stages of this experiment and for their continued interest in this work. We also thank J. Berlinghieri for his extensive assistance. We have benefited from several helpful discussions with Dr. S. Okubo and Dr. R. Thews. We particularly wish to acknowledge our frequent and essential consultations with Dr. D. Griffiths.

[24] This subtraction technique assumes that the background under the ω^0 peak in the $\pi^+\pi^-\pi^0$ mass spectrum is linear and can be adequately described by events which have the $\pi^+\pi^-\pi^0$ mass values near the position of the ω^0. The distribution in Fig. 7(f) is obtained by subtracting from the graph in Fig. 7(e) the K^+-($\pi^+\pi^-\pi^0$) mass distribution for ($\pi^+\pi^-\pi^0$) masses below and above the ω^0 peak. Figure 7(f) should, in principle, yield a more correct description of the $K^+\omega^0$ mass spectrum in reaction (6) than that given in Fig. 7(e).